

Electrical and optical properties of p-type InN

Marie A. Mayer^{1,2}, Soojeong Choi³, Oliver Bierwagen³, Holland M. Smith III^{1,2}, Eugene E.

Haller^{1,2}, James S. Speck³ and Wladek Walukiewicz¹

1. Materials Sciences Division, Lawrence Berkeley National Laboratory
2. Department of Materials Science and Engineering, University of California, Berkeley
3. Materials Department, University of California, Santa Barbara

Abstract

We have performed comprehensive studies of optical, thermoelectric and electrical properties of Mg doped InN with varying Mg doping levels and sample thicknesses. Room temperature photoluminescence spectra show a Mg acceptor related emission and the thermopower provides clear evidence for the presence of mobile holes. Although the effects of the hole transport are clearly observed in the temperature dependent electrical properties, the sign of the apparent Hall coefficient remains negative in all samples. We show that the standard model of two electrically well connected layers (n-type surface electron accumulation and p-type bulk) does not properly describe Hall effect in p-type InN.

I. Introduction

Band gaps ranging from 0.7 eV (InN) to 6.1 eV (AlN) make group III-Nitride alloys an attractive choice for numerous applications^{1,2}, but the prospects for optoelectronic devices requiring low band gap nitrides have been deterred by the presence of a highly conducting n-type layer on all InN surfaces. It is now understood that the location of the Fermi stabilization energy³ at 0.9 eV above the conduction band edge causes the surface Fermi level to be pinned above the conduction band by donor defects at the film interface and surface. These n-type

surface electron accumulation layers (SEALs) have made it impossible to directly measure bulk electrical transport properties of p-type InN^{4,6}.

Electrochemical capacitance voltage profiling (ECV) and thermopower measurements have provided convincing evidence for p-type conductivity in Mg doped InN films^{7,8}. However there is still no consensus on to what extent current can penetrate the SEAL and possible depletion region or how to interpret the Hall effect and the conductivity results in p-type InN^{7,8,9,10}. In this work, we demonstrate in a series of experiments that mobile holes contribute to the thermoelectric and electrical properties of Mg-doped InN. Although the electrical current is injected into the p-type layer, the Hall effect cannot be described in terms of two parallel conducting layers.

II. Experiment

Two sets of Mg-doped epilayers of InN were grown by plasma-assisted molecular beam epitaxy on Lumilog GaN:Fe templates with 100 nm insulating C-doped GaN buffer layers. The first set had a constant thickness of 1200 nm, but ranged in Mg concentration from 0 to $\sim 7 \times 10^{19} \text{ cm}^{-3}$ (as measured with secondary ion mass spectroscopy). In the second set, the Mg concentration for all samples was $1.5 \times 10^{19} \text{ cm}^{-3}$, but the thicknesses varied from 400 to 2400 nm. X-ray diffraction rocking curve full width half maxima (FWHM) decreased monotonically with thickness from 0.14° for the 400 nm sample to 0.12° for the 2400 nm sample. ECV measurements indicated p-type films. A nominally undoped InN film with 1200 nm thickness (FWHM of 0.14°) was used as a reference.

Variable temperature Hall effect measurements (300-5K) were done by applying currents ranging from 1-10 mA at a magnetic field of 1 Tesla. Ohmic pressed-on In contacts were used in the van der Pauw configuration. Thermopower measurements were performed in the lateral

gradient geometry using pressed-on In contacts; more detail on the setup has been provided elsewhere¹¹. Low temperature (15 K) Photoluminescence (PL) was excited with a 200 mW 488 nm Ar ion laser, dispersed with a double grating monochromator and measured with an InGaAs photodiode held at 77K.

III. Results

A. Samples with varying Mg concentration

Fig. 1 and Fig. 2 show, respectively, the PL and thermopower measurements on the set of samples with varying Mg doping. A typical, well-resolved band edge PL peak is observed at the photon energy of 0.68 eV in the undoped sample. The intensity of the peak decreases with increasing Mg doping and another lower energy peak appears at about 61 meV below the band edge emission. The additional low energy PL emission has been observed before and can be attributed to the transitions between the conduction band and the acceptor level^{7,12}. Only one PL peak, associated with the band to acceptor transition, is observed for the intermediate doping level, $9 \times 10^{17} \text{ cm}^{-3}$. No luminescence is observed in samples with higher doping levels and high positive thermopower. The result confirms previous observations⁸ that the PL is affected by the potential in the subsurface region; the potential in the depletion region between n-type surface and p-type bulk could separate the photoexcited carriers and reduce the probability for the radiative transitions.

As seen in Fig. 2, the thermopower is positive for Mg doping exceeding $4 \times 10^{18} \text{ cm}^{-3}$. It reaches a maximum for a Mg concentration of $5 \times 10^{18} \text{ cm}^{-3}$ and starts to decrease at higher doping levels. However it is still positive for a Mg doping of $7 \times 10^{19} \text{ cm}^{-3}$. The results indicate a wider range of Mg concentrations (p-type “window”) at which thermopower remains positive

than that previously reported for p-type InN⁷. The results of the thermopower measurements clearly demonstrate the presence of mobile holes in Mg-doped InN.

Despite the clear evidence for the presence of the mobile holes in Mg doped InN so far, there has been no direct confirmation of the p-type conductivity with the Hall effect measurements^{7,8}. To better understand this issue we measured temperature dependent conductivity and Hall effect. Fig. 3 shows the temperature dependent conductivity and Fig. 4 shows the apparent sheet carrier concentrations determined from the Hall coefficient measurements in the samples with variable Mg doping levels. Although all the samples have negative Hall coefficients, the samples with Mg doping levels within the p-type doping “window” showed pronounced temperature dependence. It is worth noting that the strongest temperature dependence is observed in the samples with highest positive thermopower. This confirms that mobile holes contribute to the Hall effect and that the contribution is temperature dependent with the holes freezing out at low temperature.

B. Samples with varying thickness

The overall picture of the charge transport in Mg-doped InN emerging from our results is that of an n-type SEAL enveloping a p-type bulk with well conducting mobile holes. However the question remains on how the SEAL is electrically connected to the p-type bulk and whether it is possible to deduce properties of the bulk holes from the charge transport measurements. To address this issue we grew a series of Mg doped samples with variable thickness. The Mg doping level of $1.5 \times 10^{19} \text{ cm}^{-3}$ is within the Mg concentration range (0.4×10^{19} to $2 \times 10^{19} \text{ cm}^{-3}$) that produced high positive Seebeck coefficients. The room temperature Seebeck coefficients are given in Fig. 5. As expected, the thermopower increased with increasing sample thickness, indicating still significant although diminishing contribution from the n-type SEAL. The 2400

nm thick sample had a room temperature Seebeck coefficient of $1045 \mu\text{V/K}$, which to our knowledge is highest value ever reported for p-InN. This unexpectedly large Seebeck coefficient cannot be understood in terms of the previously presented model⁷, which assumed that thermopower is determined by mobile holes located in the valence band, and will be discussed later.

The temperature dependence of the sheet resistance and the apparent sheet carrier concentration for the samples with different thickness are shown in Figs. 6 and 7, respectively. Although the contribution of p-type layer is clearly visible in the increasing temperature dependence of both resistivity and apparent carrier concentration, the striking feature of these data is that again the Hall coefficient had a negative sign in all samples. Even in the thickest sample, the contribution from the p-type bulk layer was not sufficient to change the sign of the Hall effect. As is seen in Figs. 6 and 7 the low temperature (5-70K) sheet resistances and apparent sheet electron concentrations were independent of thickness and therefore can be attributed to the contribution of the electrons in the SEAL.

IV. Analysis and discussion

It has been shown previously that charge transport in n-type InN is well described by a model with two perfectly electrically connected layers: the SEAL and the n-type bulk layer^{8,13}. On the other hand, a recent work argues through use of an ionic liquid gated device that, in the case of p-type InN, a weakly rectifying p/n junction is formed between the n-type SEAL and p-type bulk layer¹⁰. In such case, one would expect a nonzero shunt resistance that could reduce current flow through the p-type layer. It should be noted, however, that in the Hall effect or thermopower measurement configuration the contact area between SEAL and p-type layer is much larger and the effective shunt resistance can be significantly smaller.

In a simple two layer model (e.g., Petritz¹⁴), the Seebeck coefficients, mobilities and sheet conductivities are related through set of three equations:

$$\sigma = \sigma_s + \sigma_b \quad (1)$$

$$\sigma S = \sigma_s S_s + \sigma_b S_b \quad (2)$$

$$\sigma \mu = \sigma_s \mu_s + \sigma_b \mu_b \quad (3)$$

where σ , S and μ are the measured total conductivity, Seebeck coefficient and mobility, respectively whereas σ_b (σ_s), S_b (S_s) and μ_b (μ_s) refer to the bulk (surface) components of the sheet conductivity, Seebeck coefficient and mobility. Calculations used the convention of negative Seebeck coefficient and mobility for electrons. In Eqs. 1-3 the only parameter dependent on the sample thickness is the sheet conductivity of the p-type layer $\sigma_b(d) = \sigma_{bb} \cdot d$, where σ_{bb} is the volume (bulk) conductivity in cm^{-3} of the p-type layer and d is the layer thickness. Consequently, if the assumption that p-type InN transport obeys the model of two perfectly connected parallel conducting layers is correct, the quantities represented by Eqs. 1 to 3 should be linearly dependent on the thickness, d .

This analysis is shown in Figs. 8-10 as plots of the left hand side of each equation vs. the sample thickness. The values of σ (Fig. 8) as well as the product $S\sigma$ (Fig. 9) show very good linear dependencies on the sample thickness. However, in stark contrast, the quantity $\sigma\mu$ (Fig. 10) exhibits a strongly non-linear behavior. In a simple picture of two well connected layers, $\sigma\mu$ should increase with increasing thickness and change sign when the p-type layer starts to dominate the Hall effect. Instead, the $\sigma\mu$ values remain negative and saturate for larger sample thicknesses. Since, as is shown in Fig. 8, σ is a linear function of the thickness, such nonlinear behavior can be traced to an additional dependence of the effective μ that has been experimentally determined from the Hall effect measurements. Unfortunately, there is no

straightforward description of the Hall effect in such a two layer system. The main reason is that in standard Hall effect, the majority carriers are deflected by the magnetic field and accumulate on one side producing the Hall voltage with no current flowing. In the present n-type/p-type bilayer system, electrons in the n-type surface layer are deflected to the same side as holes in the p-type layer. They recombine, producing currents and additional potential drops that affect the Hall voltage and thus also the effective mobility measured on the top layer. This violates the key condition under which the Eq. 3 was derived and makes any attempts to deduce hole mobility and hole concentration from the Hall effect measurements of p-type doped InN rather difficult if not impossible.

An interesting aspect of the thermopower results shown in Fig. 5 is the large positive value of the Seebeck coefficient found in the thick Mg doped samples. The value of S larger than 1 mV/K indicates a non-degenerate hole gas with very low hole concentration, roughly 10^{16} cm^{-3} based on previous calculations. However this is inconsistent with the conductivity results which indicate considerable hole contribution to the total conductivity. The increased value of the Seebeck coefficient could be associated with additional contribution to the thermopower from high effective mass holes located in the Mg impurity band. Such explanation has been previously proposed to explain thermopower in GaAs doped with Mn acceptors¹⁵.

V. Conclusions

In conclusion, we have carried out extensive investigations of the properties of Mg doped InN. We clearly observed the electrical charge transport through bulk p-type InN despite the presence of the n-type surface electron accumulation layer. Low temperature measurements in p-type samples show definite evidence for hole freeze out and, practically, we have shown that it is possible to identify p-type InN with two Hall effect measurements, one at 300K and one at

77K. Thick Mg doped samples exhibit unexpectedly large Seebeck coefficients which we tentatively attribute to the hole transport in the partially occupied Mg acceptor band. Despite the observed large contribution of the mobile holes to the thermopower and the conductivity, the Hall effect remained negative in all studied samples. The non-linear dependence of the conductivity-mobility ($\sigma\mu$) product on sample thickness indicates that a derivation of the hole concentration and mobility assuming two parallel conducting layers model cannot be carried out in p-type InN. This behavior can be explained by presence of Hall voltage-induced currents that invalidate a standard interpretation of the Hall effect.

Acknowledgements

We would like to thank Grant Buchowicz and Oscar Dubon for assistance with Hall effect measurements and Nate Miller for construction of the thermopower apparatus. This work was supported by the Director, Office of Science, Office of Basic Energy Sciences, Materials Sciences and Engineering Division, of the U.S. Department of Energy under Contract No. DE-AC02-05CH11231.

References

- ¹ J. Wu, W. Walukiewicz, K. M. Yu, W. Shan, J. W. Ager III, E. E. Haller, H. Lu, W. J. Schaff, W. K. Metzger, and S. Kurtz, *Journal of Applied Physics* **94**, 6477 (2003).
- ² P. Schley, R. Goldhahn, G. Gobsch, M. Feneberg, K. Thonke, X. Wang, and A. Yoshikawa, *Physica Status Solidi B* **246**, 1177 (2009).
- ³ W. Walukiewicz, *Applied Physics Letters* **54**, 2094 (1989).
- ⁴ I. Mahboob, T.D. Veal, C.F. McConville, H. Lu, and W. J. Schaff, *Physical Review Letters* **92**, 036804 (2004).

- ⁵ S.X. Li, K.M. Yu, J. Wu, R. E. Jones, W. Walukiewicz, J. W. Ager, W. Shan, E. E. Haller, Hai Lu, and W. J. Schaff, *Phys. Rev. B* **71**, 161201(R) (2005).
- ⁶ T. D. Veal, L. F. J. Piper, I. Mahboob, Hai Lu, W. J. Schaff, and C. F. McConville, *Physica Status Solidi C* **2**, 2246-2249 (2005).
- ⁷ N. Miller, J. W. Ager III, H. M. Smith III, M. A. Mayer, K. M. Yu, E. E. Haller, W. Walukiewicz, W. J. Schaff, C. Gallinat, G. Koblmüller, and J. S. Speck, *Journal of Applied Physics* **107**, 113712 (2010).
- ⁸ R. E. Jones, K. M. Yu, S. X. Li, W. Walukiewicz, J.W. Ager III, E. E. Haller, H. Lu, and W. J. Schaff, *Physical Review Letters* **96**, 125505 (2006).
- ⁹ P.A. Anderson, C.H. Swartz, R. J. Reeves, D. Carder, and S. M. Durbin, *Applied Physics Letters* **89**, 184104 (2006).
- ¹⁰ E. Alarcon-Llado, M. A. Mayer, B.W. Boudouris, R.A. Segalman, N. Miller, T. Yamaguchi, K. Wang, Y. Nanishi, E.E. Haller, and J. W. Ager III, *Applied Physics Letters* **99**, 102106 (2011).
- ¹¹ J. W. Ager III, N. Miller, R. E. Jones, K. M. Yu, J. Wu, W. J. Schaff, and W. Walukiewicz, *Physical Status Solidi B* **245**, 873 (2008).
- ¹² X. Wang, S. B. Che, Y. Ishitani, and A. Yoshikawa, *Applied Physics Letters* **92**, 132108 (2008).
- ¹³ T. B. Fehlberg, G. A. Umana-Membreno, B. D. Nener, G. Parish, C. S. Gallinat, Gregor Koblmuller, S. Rajan, S. Bernardis, and J. S. Speck, *Japanese Journal of Applied Physics* **45**, L1090-L1092 (2006).
- ¹⁴ R. L. Petritz, *Physical Review* **110**, 1254 (1958).
- ¹⁵ M. A. Mayer, P. R. Stone, N. Miller, H. M. Smith III, O. D. Dubon, E. E. Haller, K. M. Yu, W. Walukiewicz, X. Liu, and J. K. Furdyna, *Physical Review B* **81**, 045205 (2010).

Figure 1. (Color online) Photoluminescence spectroscopy measured at 15 K on p-InN samples with various Mg concentrations using an Ar ion laser and InGaAs photodiode detector.

Figure 2. (Color online) Room temperature thermopower of p-InN as a function of Mg concentration.

Figure 3. (Color online) Sheet resistance as a function of temperature for 1200 nm InN samples with varying Mg concentration. 1200 nm undoped, n-type InN reference sample included.

Figure 4. (Color online) Apparent carrier sheet concentration as a function of temperature for InN samples with varying Mg concentrations. Inset shows mobility values as a function of Mg concentration at low and high temperatures.

Figure 5. (Color online) Room temperature thermopower of p-InN as a function of thickness.

Figure 6. (Color online) Sheet resistance as a function of temperature for p-type InN samples with varying thickness and Mg concentration of $1.5 \times 10^{19} \text{ cm}^{-3}$. 1200 nm undoped, n-type InN reference sample included. Inset shows mobility values as a function of thickness at low and high temperatures.

Figure 7. (Color online) Apparent carrier sheet concentration as a function of temperature for p-type InN samples with varying thickness and a 1200 nm undoped InN sample.

Figure 8. (Color online) Sheet conductivity (σ_{sheet}) vs. thickness (d) for four p-type InN samples (Eqn 1). Linear fit with extremely high correlation coefficient shown.

Figure 9. (Color online) Sheet conductivity (σ_{sheet}) x thermopower (S) vs. thickness (Eqn. 2). Linear fit with extremely high correlation coefficient shown.

Figure 10. (Color online) Sheet conductivity (σ_{sheet}) x mobility (μ) vs. thickness (Eqn. 3).

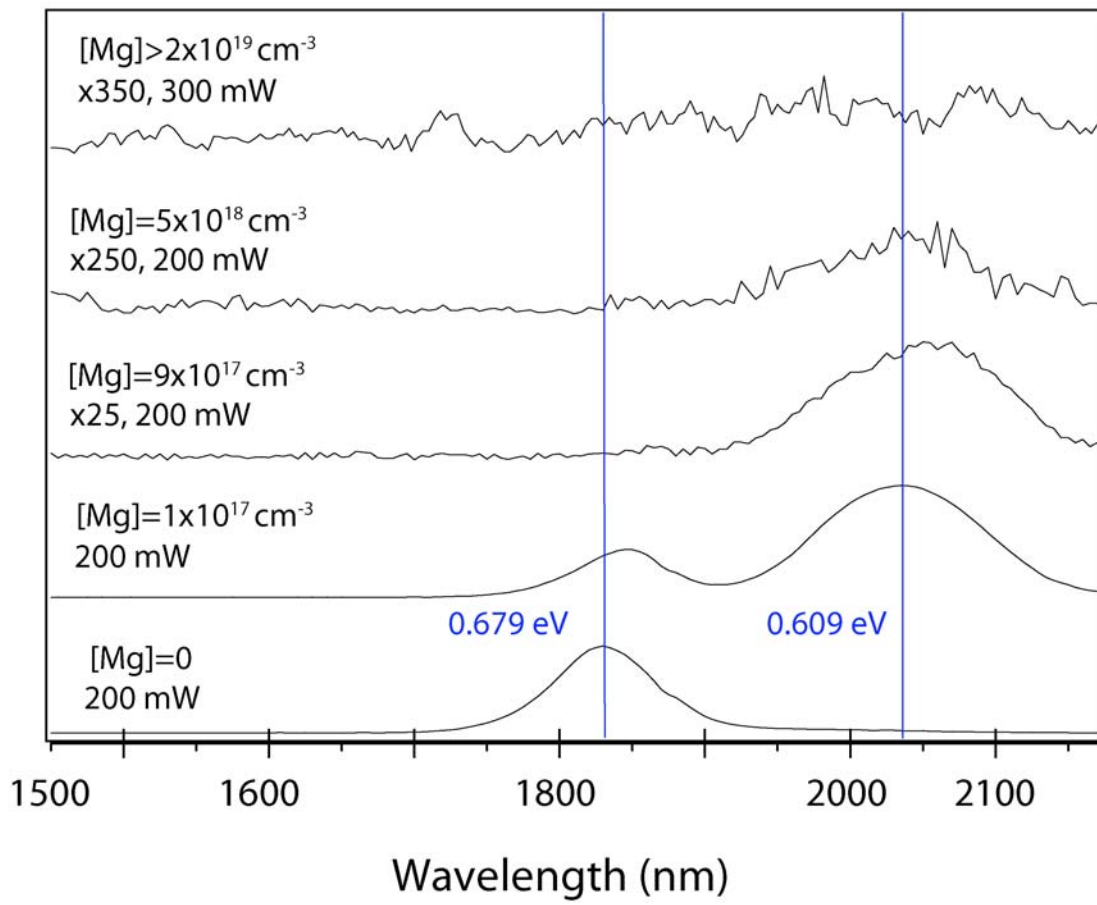


Figure 1

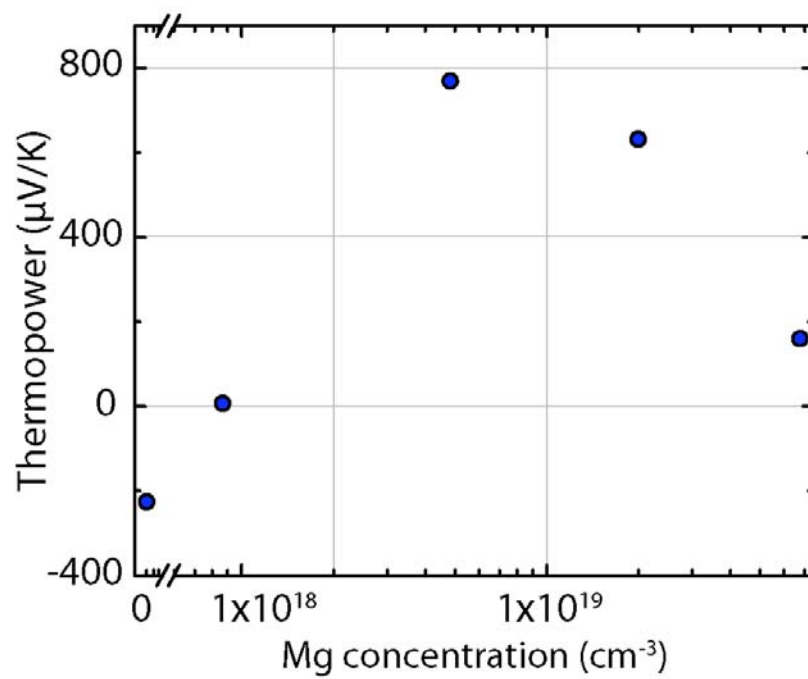


Figure 2

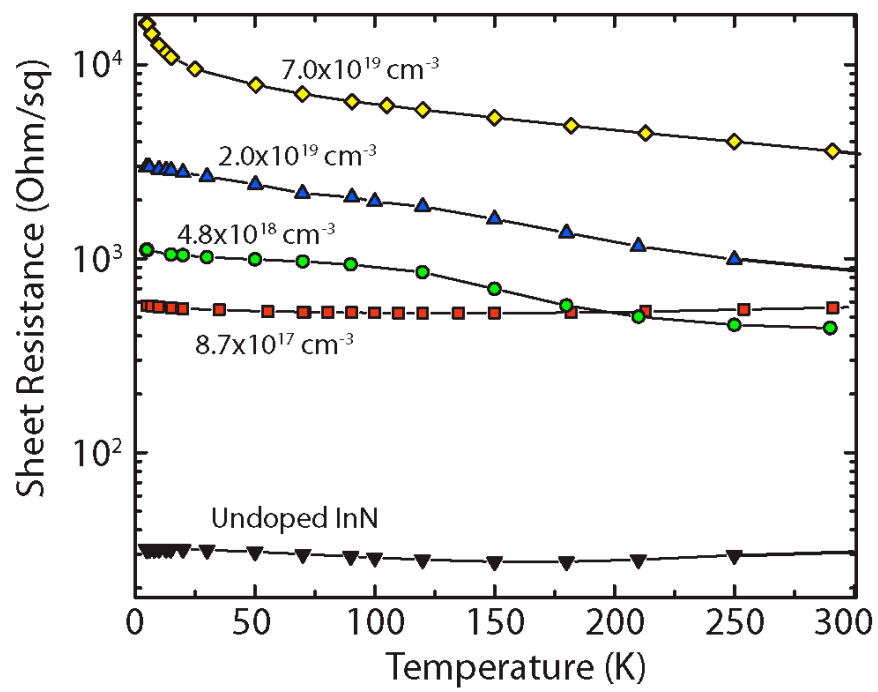


Figure 3

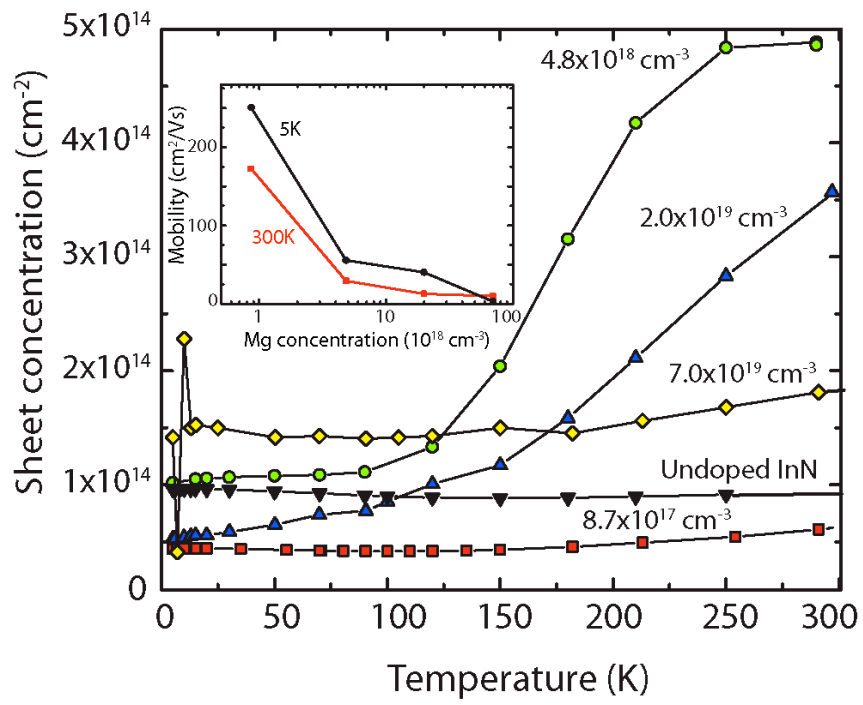


Figure 4

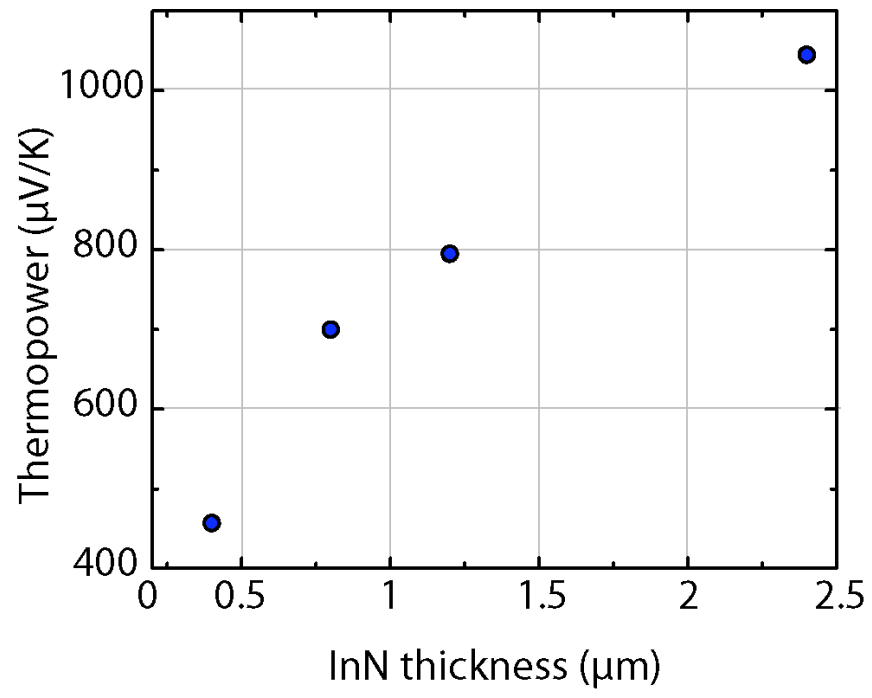


Figure 5

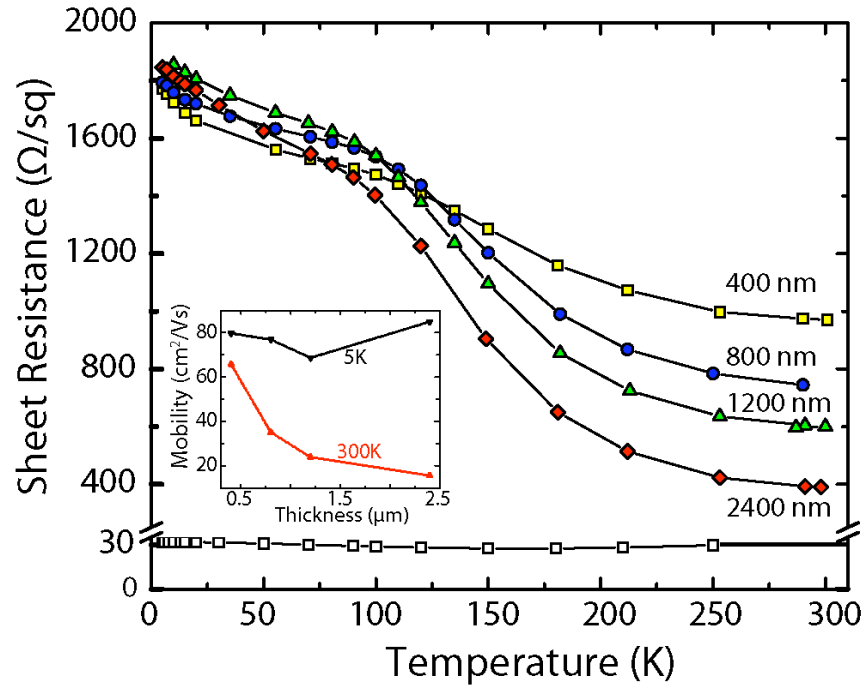


Figure 6

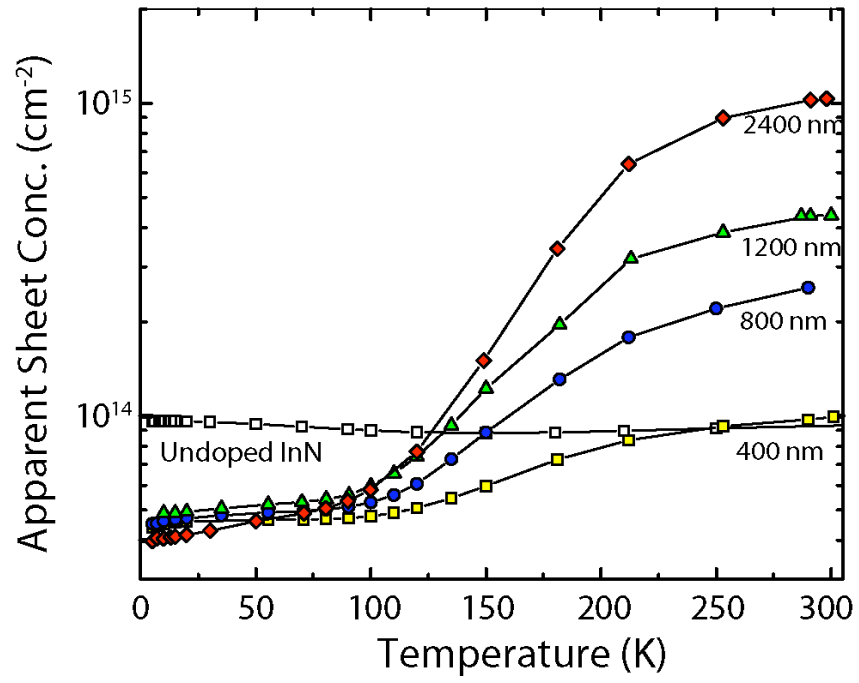


Figure 7

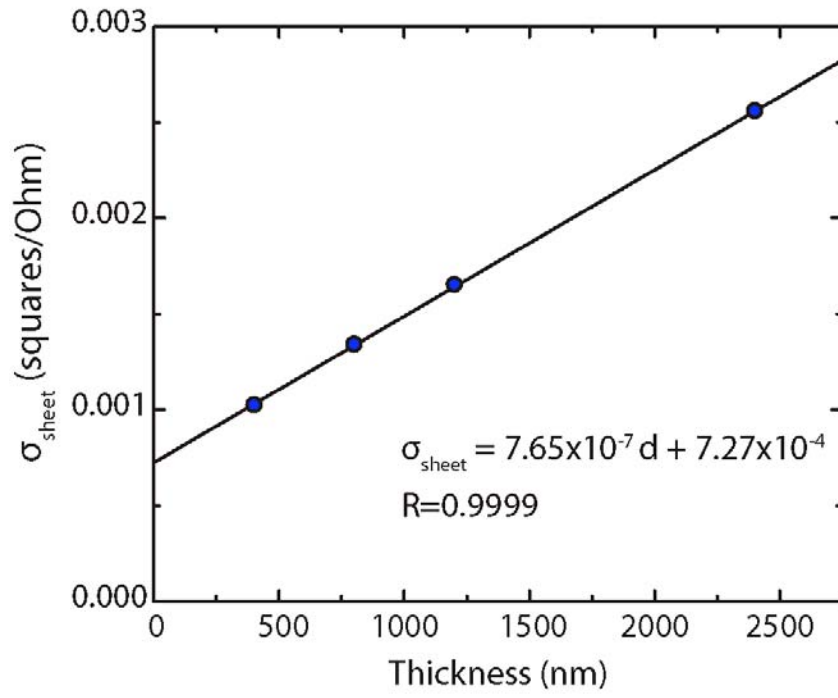


Figure 8

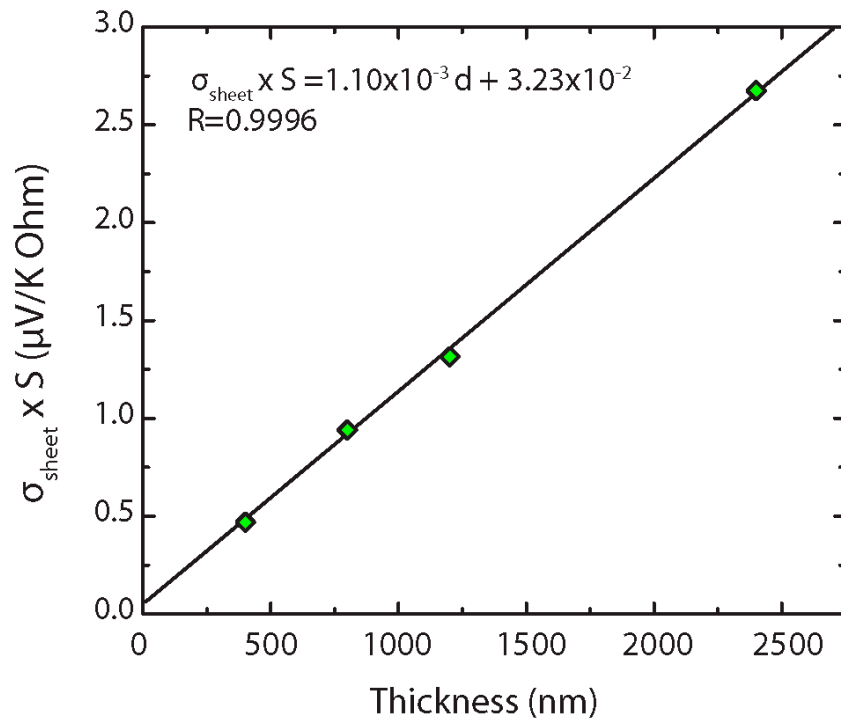


Figure 9

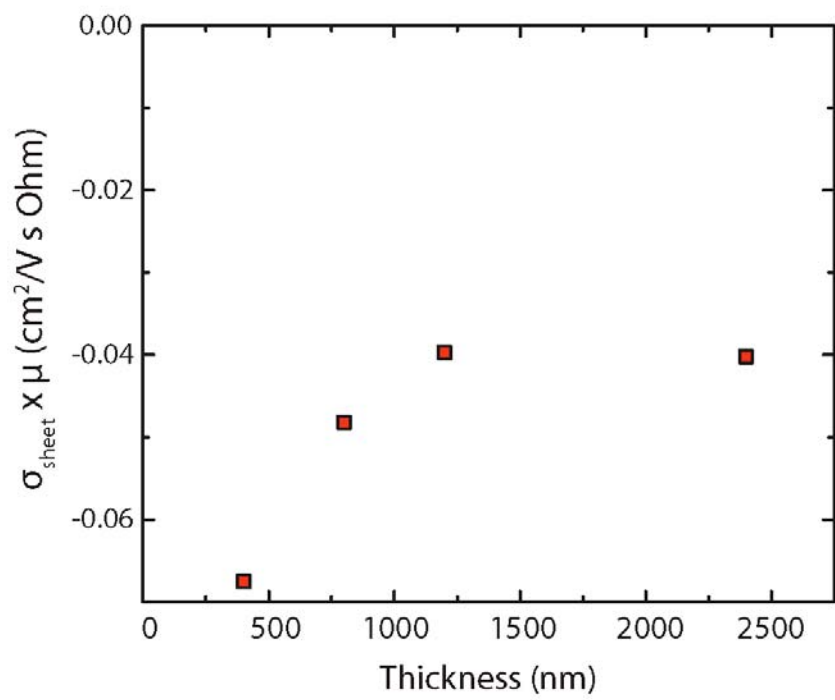


Figure 10

DISCLAIMER

This document was prepared as an account of work sponsored by the United States Government. While this document is believed to contain correct information, neither the United States Government nor any agency thereof, nor The Regents of the University of California, nor any of their employees, makes any warranty, express or implied, or assumes any legal responsibility for the accuracy, completeness, or usefulness of any information, apparatus, product, or process disclosed, or represents that its use would not infringe privately owned rights. Reference herein to any specific commercial product, process, or service by its trade name, trademark, manufacturer, or otherwise, does not necessarily constitute or imply its endorsement, recommendation, or favoring by the United States Government or any agency thereof, or The Regents of the University of California. The views and opinions of authors expressed herein do not necessarily state or reflect those of the United States Government or any agency thereof or The Regents of the University of California.